Dyes and Pigments 94 (2012) 66–73

Contents lists available at SciVerse ScienceDirect

Dyes and Pigments

journal homepage: www.elsevier.com/locate/dyepig

# Synthesis and photophysical properties of covalently linked boron dipyrromethene dyads

Tamanna K. Khan [a], Mushtaque S. Shaikh [b], M. Ravikanth [a,*]

[a] Department of Chemistry, Indian Institute of Technology, Powai, Mumbai 400076, India
[b] Department of Pharmaceutical Chemistry, Bombay College of Pharmacy, Santacruz (E), Mumbai 400098, India

ARTICLE INFO

*Article history:*
Received 24 October 2011
Received in revised form
1 December 2011
Accepted 4 December 2011
Available online 11 December 2011

*Keywords:*
*Meso*-furyl boron dipyrromethenes
Easier reductions
Boron dipyrromethene dyads
Energy transfer
DFT
TDDFT

ABSTRACT

Two covalently linked boron dipyrromethene (BODIPY) dyads containing *meso*-phenyl BODIPY and *meso*-furyl BODIPY units connected via *meso-meso* and *meso*-α positions were synthesized by a Pd(0) coupling reaction. The dyads are freely soluble in common organic solvents and their structures were confirmed by HR-MS, 1D and 2D NMR techniques. Absorption studies indicate that the *meso*-aryl BODIPY and the *meso*-furyl BODIPY absorb in two different regions and that the *meso*-furyl BODIPY absorbs at lower energy compared to the *meso*-aryl BODIPY. The steady state fluorescence studies carried out by exciting the *meso*-aryl BODIPY unit clearly indicated an efficient singlet–singlet energy transfer from the *meso*-aryl BODIPY unit to *meso*-furyl BODIPY unit in both dyads. Furthermore the *meso*-α linked BODIPY dyad ($\phi_f = 0.41$) is more fluorescent than its corresponding BODIPY monomers whereas the *meso-meso* linked BODIPY dyad ($\phi_f = 0.017$) is weakly fluorescent. This unexpected observation was tentatively attributed to the restricted rotation of the BODIPY units in the *meso*-α linked dyad resulting in enhancement of radiative transitions. The time-resolved fluorescence study also indicated that *meso*-α linked BODIPY dyad is more fluorescent with singlet state lifetime of 3.7 ns. The DFT studies carried out on dyads are in agreement with the experimental observations.



## 1. Introduction

The importance of photosynthesis has driven many researchers to look for ways to duplicate the fundamental features of photosynthesis, i.e. energy transfer and electron transfer in simplified systems. The light-harvesting system, which absorbs light and funnels energy to the reaction center by a series of energy transfer steps, plays a very important role in photosynthesis [1]. An ideal light-harvesting system that mimics photosynthesis process should have the ability to absorb light efficiently in a relatively broad region and to achieve this, the combination of multiple chromophores is necessary. The development of highly efficient light-harvesting systems remains a challenging task as many aspects require improvement, such as the choice of the chromophores with appropriate spectral overlap and matched energy levels, linking units, connection sites, and synthesis strategy.

4,4-Difluoro-4-bora-3a,4a-diaza-*s*-indacene (BODIPY) chromophores have received significant interest due to their outstanding optical properties such as high absorption coefficients and relatively sharp emission bands, high fluorescence quantum yields, excellent chemical and photochemical stability, high solubility, and ease of functionalization [2–4]. BODIPY dyes connected to other chromophores such as porphyrin [5–8], pyrene [9,10], anthracene [11], BODIPY [12] and Zn(II)/Ru(II) terpyridine [13–15] have been synthesized and their singlet–singlet energy transfer properties explored. Depending on the other chromophore to which the BODIPY unit is connected, the BODIPY unit in BODIPY–chromophore conjugates can act as either the energy donor or energy acceptor. Since the properties of the BODIPY unit can be fine tuned at will by suitable substitution, there have been some recent reports concerning BODIPY arrays containing two or more BODIPY units which demonstrate the possibility of energy transfer from one BODIPY unit to another BODIPY unit (Chart 1). For example, Akkaya and co-workers synthesized BODIPY tetrad **1** in which two BODIPY units are covalently linked at the 3,5-positions of another BODIPY via styryl linker which in turn linked to the fourth BODIPY through the *meso*-phenyl [16]. Zhang and co-workers synthesized a BODIPY triad **2** composed of three kinds of BODIPY units [17]. Recently, Ziessel and co-workers synthesized a panchromatic BODIPY array **3** in which five BODIPY units are covalently linked in an iterative fashion [18]. The same group also reported a star-shaped supramolecular system containing three different BODIPY dyes **4**

* Corresponding author. Tel.: +91 22 5767176; fax: +91 22 5723480.
*E-mail address:* ravikanth@chem.iitb.ac.in (M. Ravikanth).

0143-7208/$ – see front matter © 2011 Elsevier Ltd. All rights reserved.
doi:10.1016/j.dyepig.2011.12.002

arranged around a truxene core [19]. In all these cases, the singlet state energy levels of BODIPY units are arranged in a cascade manner for efficient intramolecular energy flow from a BODIPY unit which is at high energy to the BODIPY unit which is at lower in energy. Thus, to create an energy gradient between the BODIPY units in a BODIPY array, one has to use appropriate BODIPY units whose energy levels are arranged in a favorable manner. Recently, Churchill and co-workers showed that introduction of furyl group at the *meso*-position in a BODIPY unit alters the electronic properties significantly and *meso*-furyl BODIPY absorb at lower energy compared to *meso*-phenyl BODIPY [20]. Furthermore, the *meso*-furyl BODIPY possesses a large Stokes shift compared to *meso*-phenyl BODIPY [20,21]. Since *meso*-phenyl BODIPY and *meso*-furyl BODIPY possess interesting and complementary photophysical properties, an assembly like dyad containing these two units would be helpful to study the singlet–singlet energy transfer properties. Here, we report the synthesis of two covalently linked BODIPY dyads **5** and **6** containing *meso*-aryl BODIPY and *meso*-furyl BODIPY units using readily available appropriate building blocks and demonstrate the possibility of efficient singlet–singlet energy transfer from *meso*-aryl BODIPY unit to *meso*-furyl BODIPY unit in both these dyads.

## 2. Experimental section

### 2.1. General

Compound **9** was prepared by following the literature method [11]. THF and toluene were dried over sodium benzophenone ketyl and chloroform, ethyl acetate, methanol, acetonitrile dried over calcium hydride distilled prior to use. $BF_3{\cdot}OEt_2$ and 2,3-dichloro-5,6-dicyano-1,4-benzoquinone (DDQ) obtained from Spectrochem (India) were used as obtained. All other chemicals used for the synthesis were reagent grade unless otherwise specified. Column chromatography was performed on silica (60–120 mesh).

### 2.2. Instrumentation

$^1$H NMR spectra ($\delta$ in ppm) were recorded using Varian VXR 300 and 400 MHz and Bruker 400 MHz NMR spectrometer. $^{13}$C NMR spectra were recorded on Varian and Bruker spectrometer operating at 100.6 MHz. $^{19}$F NMR spectra were recorded on Varian and spectrometer operating at 282.2 MHz. $^{11}$B NMR spectra were recorded on Varian spectrometer operating at 96.3 MHz. TMS was used as an internal reference for recording $^1$H (of residual proton;

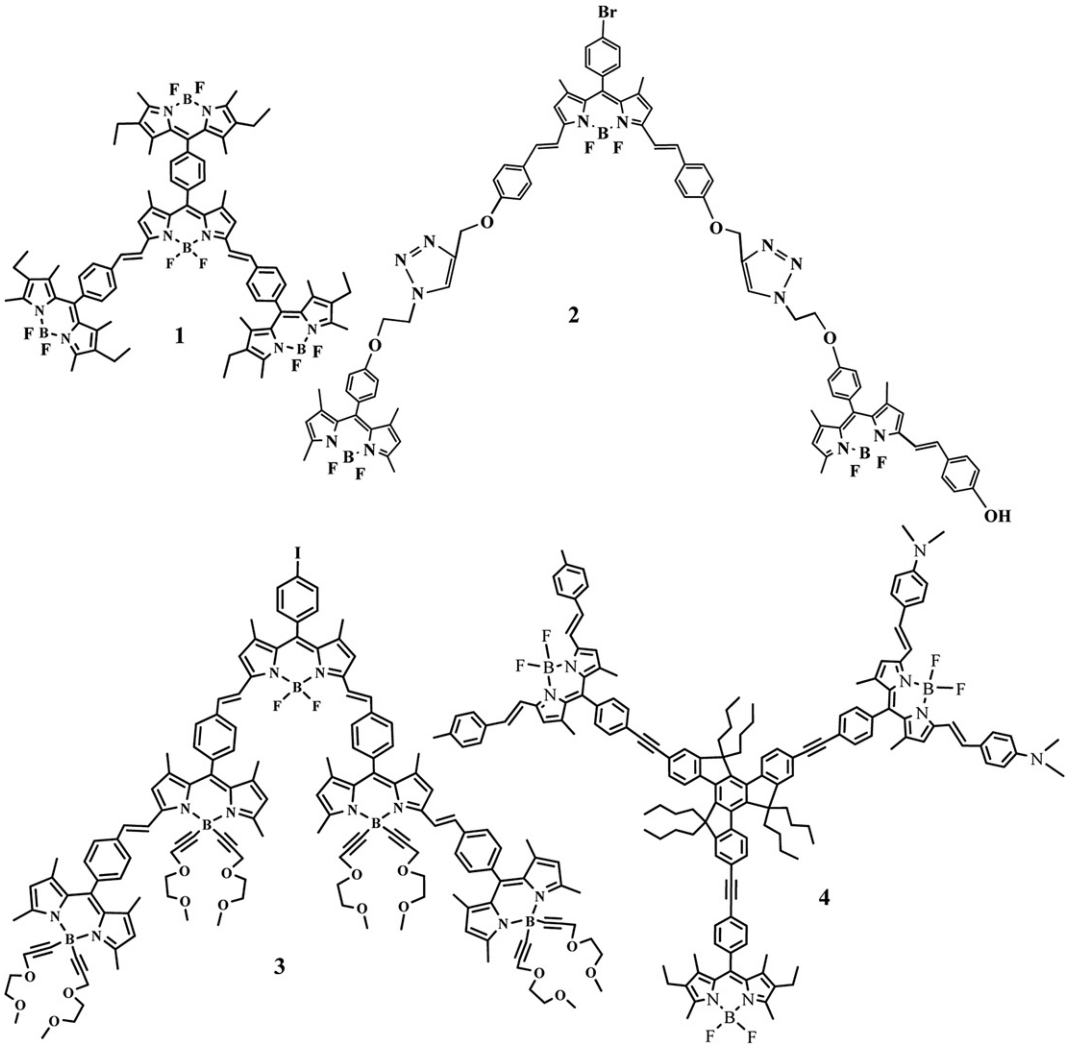


**Chart 1.** Structures of previously reported multi BODIPY systems **1**, **2**, **3** and **4**.

$\delta$ 7.26) and $^{13}C$ ($\delta$ 77.0 signal) in $CDCl_3$. Absorption and steady state fluorescence spectra were obtained with Perkin–Elmer Lambda-35 and PC1 Photon Counting Spectrofluorometer manufactured by ISS, USA instruments respectively. Fluorescence spectra were recorded at 25 °C in a 1 cm quartz fluorescence cuvette. The fluorescence quantum yields ($\Phi_f$) were estimated from the emission and absorption spectra by comparative methods at the excitation wavelength of 488 nm using Rhodamine 6G ($\Phi_f = 0.88$) [29] as standard. Cyclic voltammetric (CV) and differential pulse voltammetric (DPV) studies were carried out with an electrochemical system utilizing the three electrode configuration consisting of a glassy carbon (working electrode), platinum wire (auxiliary electrode) and saturated calomel (reference electrode) electrodes. The experiments were performed in dry dichloromethane using 0.1 M tetrabutylammonium perchlorate as supporting electrolyte. Half wave potentials were measured using DPV and also calculated manually by taking the average of the cathodic and anodic peak potentials. High-resolution mass spectra were obtained from Q-TOF instrument by electron spray ionization (ESI) technique.

### 2.3. Computational studies

The computational studies were performed with the *Jaguar* [30] application available in *Schrödinger* suit installed in Linux based operating system on a computer cluster equipped with *Rocks cluster* [31] tool. The structures of the dyads (compounds **5** and **6**) were generated *in silico* by attaching *meso*-phenyl and *meso*-2-furyl BODIPY moieties. The structures of the two parent compounds were extracted from the X-ray diffraction output files generated by Wagner [32] and Kim et al. [20], respectively. The structures were energy optimized using quantum mechanics with density functional theory (DFT) [23] and B3LYP [33] gradient corrected correlation functional method in conjugation with standard 6–31 G (p,d) basis set [34] and parameters. For the optimized structures full population analyses studies were done. In order to understand the process of energy transfer in the dyad system, their optimized structures were split into two molecules such that each fragment is attached with the linker acetylene group. The fragmented systems were also subjected to energy optimization with aforementioned protocols and population analysis. The excited state calculations were also performed for the singlet state of all the molecules and fragments with CIS method of Time-Dependent Density Functional Theory (TDDFT) [26] in *Jaguar*.

### 2.4. General procedure for the synthesis of BODIPY dyads *5*–*6*

The appropriate bromo BODIPY (**7** or **8**) and *meso*-(4-ethynyl phenyl) BODIPY **9** were dissolved in dry toluene/$Et_3N$ (6 mL, 5:1) in 25 mL, two-necked, round-bottomed flask fitted with a reflux condenser, gas inlet and gas outlet tubes for nitrogen purging. The reaction flask was placed in an oil bath preheated to 35 °C. After purging the flask with nitrogen for 15 min, $AsPh_3$ (3.5 equiv.) and $Pd_2(dba)_3$ (0.44 equiv.) were added, and the reaction mixture was stirred at 35 °C for 2 h. TLC analysis of the reaction mixture indicated the appearance of an intense new spot apart from the two minor spots corresponding to starting precursors. The solvent was removed under reduced pressure, and the crude compound was purified by column chromatography. The excess $AsPh_3$ and the small amounts of unreacted starting precursors were removed with

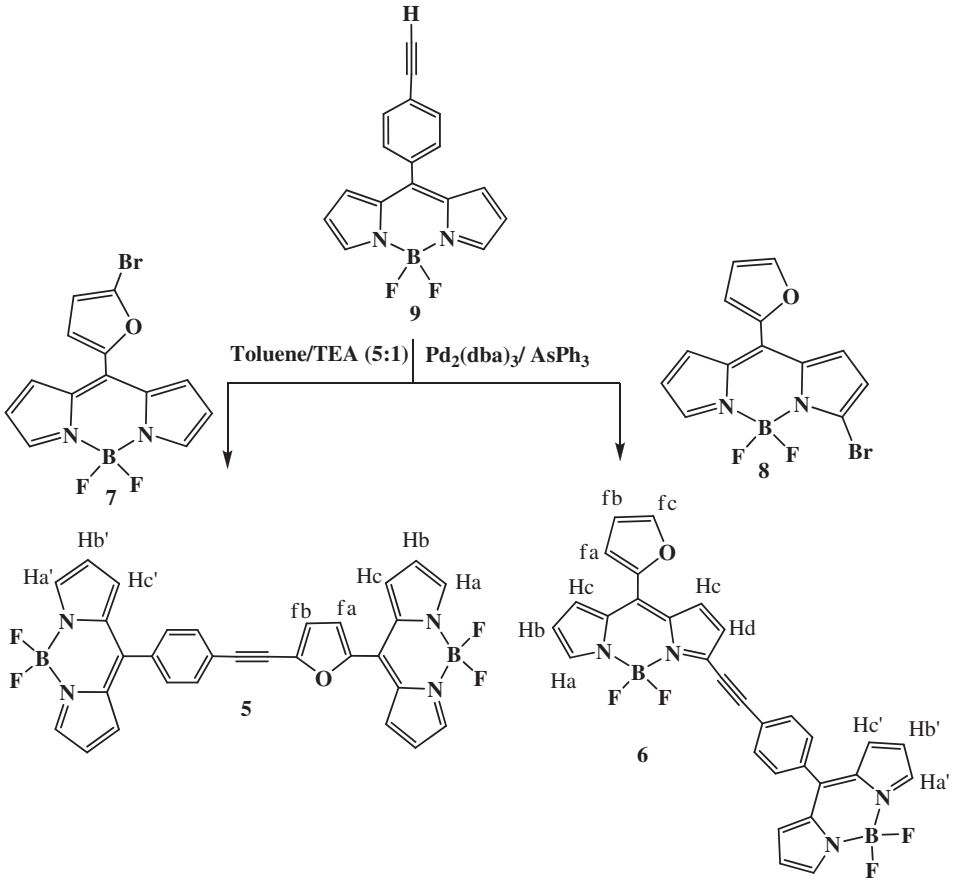


**Scheme 1.** Synthesis of BODIPY dyads **5** and **6**.

petroleum ether and the required pure BODIPY–BODIPY dyads were then collected with petroleum ether/$CH_2Cl_2$.

*2.4.1. BODIPY dyad **5***

BODIPY dyad **5** was synthesized from BODIPYs **7** and **9** after elution from an alumina column (petroleum ether/dichloromethane 75:25) 40% yield, $^1$H NMR (400 MHz, $CDCl_3$): 6.57 (d, $J = 3.0$ Hz, 2H, β-Py), 6.61 (dd, $J = 4.08$ Hz, 2H, β-Py), 6.93 (d, $J = 4.2$ Hz, 2H, β-Py), 6.99 (d, $J = 3.7$ Hz, 1H, furan), 7.26 (m, 1H, furan), 7.52 (d, $J = 4.2$ Hz, 2H), 7.61 (d, $J = 8.3$ Hz, 2H, Ar), 7.74 (d, $J = 8.2$ Hz, 2H, Ar), 7.92 (s, 2H, β-Py), 7.95 (s, 2H, β-Py). $^{13}$C NMR (100 MHz, $CDCl_3$, $\delta$ in ppm): 81.29, 96.42, 118.78, 119.08, 121.62, 124.16, 125.60, 128.57, 128.82, 129.15, 130.69, 130.86, 131.50, 131.84, 132.49, 133.89, 134.97, 134.85, 139.80, 141.58, 143.51, 143.64, 144.85, 145.96, 149.62. $^{19}$F NMR (282.2 MHz, $CDCl_3$, $\delta$ in ppm): −144.9 (q, $J_{B-F} = 57.6$ Hz), −145.6 (q, $J_{B-F} = 56.5$ Hz). $^{11}$B NMR (96.3 MHz, $CDCl_3$, $\delta$ in ppm): 0.56 (dt, $J_{B-F} = 29.5$ Hz). HR-MS mass calcd. for ($C_{30}H_{18}B_2F_4N_4O$): 529.1619 $[M - 19]^+$ found: 529.1629 $[M - 19]^+$.

*2.4.2. BODIPY dyad **6***

BODIPY dyad **6** was synthesized from BODIPYs **8** and **9** after elution from silica gel column (petroleum ether/dichloromethane 90:10) 37% yield; $^1$H NMR (400 MHz, $CDCl_3$): 6.57 (s, 2H, β-Py), 6.64 (m, 1H, β-Py), 6.74 (m, 1H, furan), 6.81 (d, $J = 4.0$ Hz, 1H, β-Py), 6.94 (d, $J = 3.6$ Hz, 2H, β-Py), 7.19 (d, $J = 3.2$ Hz, 1 H, furan), 7.48 (d, $J = 3.6$ Hz, 2 H, β-Py), 7.59 (d, $J = 8.0$ Hz, 2 H, Ar), 7.81 (d, $J = 8.0$ Hz, 2H, Ar), 7.86 (s, 1H, furan), 7.96 (s, 3H, β-Py). $^{13}$C NMR (100 MHz, $CDCl_3$, $\delta$ in ppm): 85.56, 100.32, 113.67, 119.00, 119.32, 120.67, 123.51, 125.26, 130.02, 130.77, 131.07, 131.40, 131.60, 132.26, 132.72, 133.28, 133.80, 134.72, 134.91, 135.63, 144.63, 146.40, 147.93, 148.83. $^{19}$F NMR (282.2 MHz, $CDCl_3$, $\delta$ in ppm): −145.9 (q, $J_{B-F} = 57.2$ Hz), −146.2 (q, $J_{B-F} = 56.2$ Hz). $^{11}$B NMR (96.3 MHz, $CDCl_3$, $\delta$ in ppm): 0.68 (dt, $J_{B-F} = 26.9$ Hz). HR-MS mass calcd. for ($C_{30}H_{18}B_2F_4N_4O$): 529.1619 $[M - 19]^+$ found: 529.1642 $[M - 19]^+$.

## 3. Results and discussion

The desired boron dipyrromethene building blocks such as 4,4-difluoro-8-(5-bromo-2-furyl)-4-bora-3a,4a-diaza-*s*-indacene **7**, 3-bromo-8-(2-furyl)-4-bora-3a,4a-diaza-*s*-indacene **8** and *meso*-(4-ethynyl phenyl) BODIPY **9** were synthesized by following the literature methods [11,22]. Compounds **7** and **8** were used to synthesize two BODIPY dyads **5** and **6** as shown in Scheme 1. The dyads **5** and **6** were synthesized by coupling **9** with **7** and **8**,

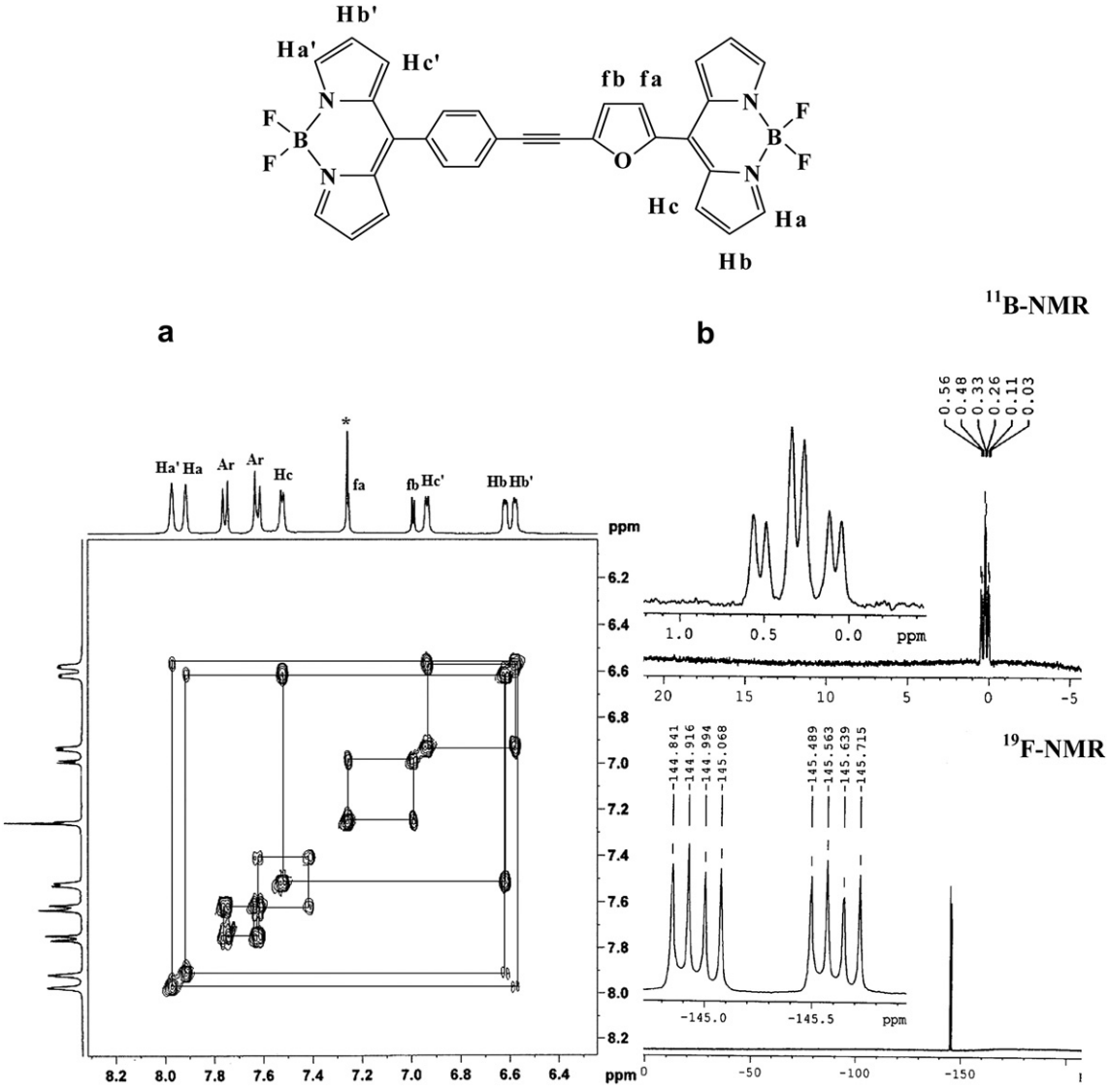


**Fig. 1.** (a) $^1$H–$^1$H COSY NMR spectrum for dyad **5** recorded in $CDCl_3$. (b) $^{11}$B and $^{19}$F NMR spectra for dyad **5** recorded in $CDCl_3$.

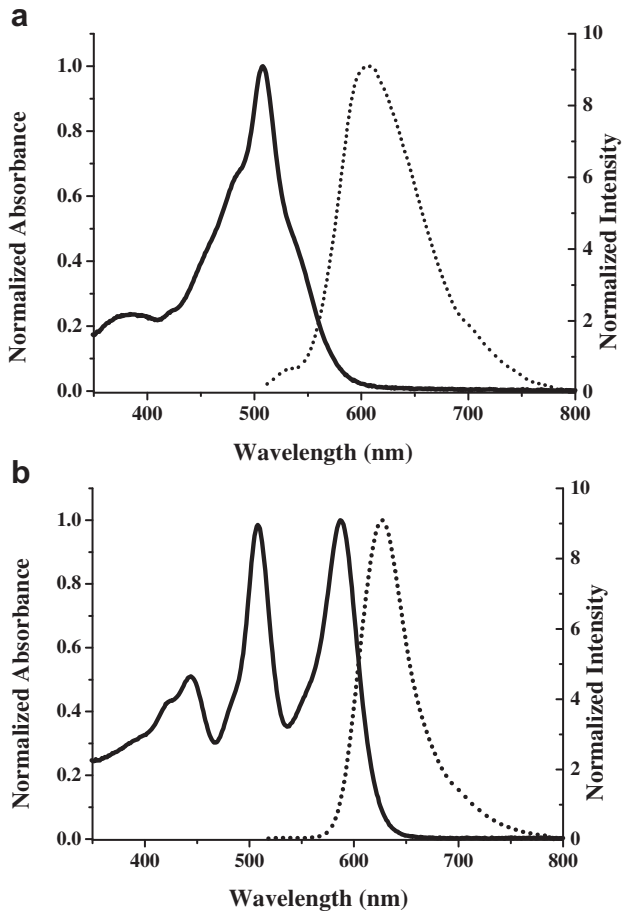


**Fig. 2.** Normalized absorption (—) and emission (…) spectra of (a) **5** and (b) **6** recorded in toluene.

respectively, in toluene/triethylamine in the presence of $AsPh_3$/$Pd_2(dba)_3$ at 35 °C for 2 h. The crude mixtures were purified by column chromatography and afforded pure dyads **5** and **6** in 40% and 37% yields, respectively. The compounds **5** and **6** were confirmed by HR-MS and characterized in detail by $^1H$, $^{19}F$ and $^{11}B$ along with $^1H-^1H$ COSY NMR spectroscopy. The protons of two different BODIPY units in dyads **5** and **6** were easily identified by close inspection of their $^1H-^1H$ COSY NMR spectra presented for compound **5** in Fig. 1. Churchill et al. [20] have shown that *meso*-furyl BODIPY exhibit the pyrrole proton signals at slightly lower field compared to *meso*-aryl BODIPYs. This is due to enhanced conjugation in *meso*-furyl BODIPY due to more in-plane orientation of *meso*-furyl group with BODIPY core unlike *meso*-aryl BODIPYs in which the *meso*-aryl group is inclined more toward orthogonal to BODIPY core. In compound **5**, the pyrrole protons Ha, Hb and Hc of *meso*-furyl BODIPY unit appeared as three sets of signals at lower field compared to the pyrrole protons Ha′, Hb′ and Hc′ of *meso*-aryl BODIPY unit (Fig. 1a). These protons were identified with the help of cross peaks observed in $^1H-^1H$ COSY NMR spectrum. Similarly, the furyl protons fa and fb also identified at 6.99 and 7.26 ppm, respectively, by $^1H-^1H$ COSY NMR spectrum (Fig. 1a). Compound **6** showed slightly different NMR features compared to **5** because of the difference of linking of *meso*-aryl and *meso*-furyl BODIPYs. Due to unsymmetrical linking, five sets of pyrrole signals were observed for *meso*-furyl BODIPY unit and three sets of pyrrole signals for *meso*-aryl BODIPY unit in compound **6** (Supporting information). Furthermore, the pyrrole protons in compound **6** were observed at slightly lower field compared to compound **5**. In the $^{19}F$ NMR spectra of compounds **5** and **6**, due to the presence of two different types of *meso*-substituted BODIPY units, two sets of quartets at approximately −145 ppm with almost no shift in their chemical shifts compared to their monomers were observed. Similarly, two overlapping triplets at ~0.5 ppm in $^{11}B$ NMR spectra were observed due to the presence of *meso*-aryl and *meso*-furyl BODIPYs in compounds **5** and **6**.

The properties of dyads **5** and **6** were studied by absorption, fluorescence and electrochemical techniques. The normalized absorption spectra for compounds **5** and **6** are shown in Fig. 2 and the relevant data along with *meso*-phenyl and *meso*-furyl BODIPY monomers **9** and **7**, respectively, are presented in Table 1. The inspection of absorption spectra of dyads **5** and **6** showed strong $S_0 \rightarrow S_1$ transition at lower energy and a weak $S_0 \rightarrow S_2$ transition at higher energy like their corresponding BODIPY monomers. The absorption spectrum of dyad **5** showed a strong absorption band at 508 nm with an ill-defined shoulder at 537 nm. The strong band at 508 nm was exclusively due to the *meso*-aryl BODIPY unit and the weak ill-defined band was due to the *meso*-furyl BODIPY unit. However, in dyad **6**, because of the difference in linking of two BODIPY units, two well separated absorption bands were observed at 508 and 587 nm corresponding to the *meso*-aryl BODIPY unit and the *meso*-furyl BODIPY unit, respectively. Thus, in dyad **6**, the two BODIPY units clearly absorb at two different regions which helps in selective excitation of one of the BODIPY unit to study energy transfer from one BODIPY unit to the other BODIPY unit.

The electrochemical studies of dyads **5** and **6** were undertaken in $CH_2Cl_2$ using TBAP as supporting electrolyte at different scan speeds. The dyads **5** and **6** showed two reductions but oxidations were not observed under our experimental conditions. For example, the dyad **5** showed three reductions at −0.30 and −0.45 (Fig. 3). In this, the reduction at −0.30 V was mainly due to the *meso*-furyl BODIPY unit since *meso*-furyl BODIPYs are easier to reduce compared to the *meso*-aryl BODIPYs; the reduction at −0.45 V was due to the *meso*-aryl BODIPY. Similar observations were found for dyad **6**. Thus, the electrochemical studies indicate that the two BODIPY units in the dyads exhibit different electrochemical behavior.

Since in dyads **5** and **6**, the *meso*-aryl BODIPY unit absorbs at higher energy and *meso*-furyl BODIPY unit [20] absorbs at lower energy, the singlet−singlet energy transfer properties from the

**Table 1**
Photophysical and Electrochemical data of BODIPY dyads **5** and **6** along with associated reference compounds recorded in toluene.

| C. No. | Photophysical data | | | | | | Electrochemical data | |
|---|---|---|---|---|---|---|---|---|
| | $\lambda_{abs}$ (nm) (log $\varepsilon$) | $\lambda_{em}$ (nm) | $\phi^d$ | $\phi^a$ | $\tau^d$ (ns) | $\tau^a$ (ns) | Reduction $E^{red}_{1/2}$ (V) ($\Delta E_p$, mV) | |
| 9 | 476 (sh) 502 (4.6) | 520 | 0.053 | | 5.0 | | | −0.78 |
| 7 | 493 (sh) 525 (4.4) | 573 | | 0.058 | | 2.60 | −0.62 | |
| 5 | 484 (sh) 508 (4.2) 537 (sh) | 603 | $<10^{-4}$ | 0.017 | | 0.60 | −0.30 | −0.45 |
| 6 | 444 (4.0) 508 (4.3) 587 (4.3) | 627 | $<10^{-4}$ | 0.41 | | 3.73 | −0.34 | −0.55 |

Note: d and a refer to donor and acceptor unit.

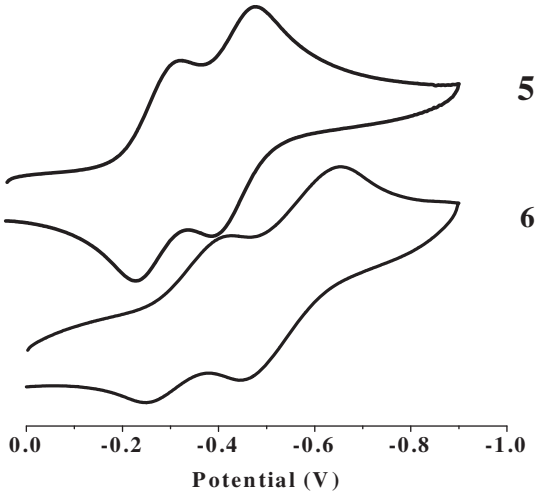


**Fig. 3.** Reduction waves of dyads **5** and **6** recorded in $CH_2Cl_2$ containing 0.1 M TBAP as the supporting electrolyte recorded at a scan speed of 50 mV/s.

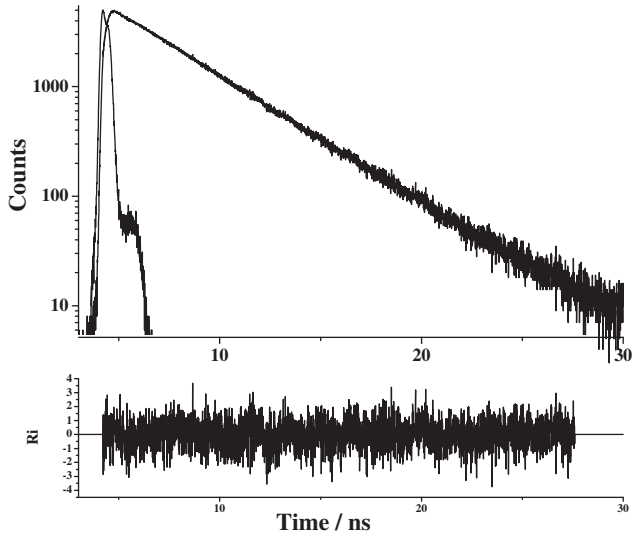


**Fig. 4.** Fluorescence decay profile along with weighted residual distribution fit for compound **6** in $CHCl_3$. The excitation wavelength used was 444 nm and emission was detected at 630 nm.

*meso*-aryl BODIPY unit to the *meso*-furyl BODIPY unit were studied using both steady state and time-resolved fluorescence techniques. In dyad **5**, on excitation at 488 nm where the *meso*-aryl BODIPY unit absorbs strongly, the emission at 525 nm due to the *meso*-aryl BODIPY was completely quenched and a strong emission was noted at 603 nm which is due to the *meso*-furyl BODIPY (Fig. 2a). Similarly, the dyad **6** which showed two clear absorption bands at 508 and 587 nm corresponding to the *meso*-phenyl BODIPY and *meso*-furyl BODIPY units, respectively, on excitation at 508 nm, the emission from *meso*-aryl BODIPY unit was quenched completely and a strong emission due to the *meso*-furyl BODIPY was observed at 630 nm (Fig. 2b). Under these experimental conditions, the 1:1 mixture of corresponding monomers of dyads **5** and **6** has shown emission exclusively from the *meso*-aryl BODIPY (Supporting information). The excitation spectra of dyads **5** and **6** recorded at their respective emission wavelengths showed absorption features of both BODIPY units. All these observations suggest that in dyads **5** and **6**, there is a possibility of singlet–singlet energy transfer from the *meso*-aryl BODIPY unit to the *meso*-furyl BODIPY unit. Furthermore, the quantum yield data of dyads **5** and **6** indicated that the dyad **6** is strongly fluorescent with a quantum yield of 0.41 whereas the dyad **5** is weakly fluorescent ($\Phi_f = 0.017$) which is also noted in their solution color under UV radiation (Supporting information). These observations were further supported by time-resolved fluorescence studies. The dyads **5** and **6** were excited at 444 nm and monitored at 603 and 630 nm, respectively, where the acceptor *meso*-furyl BODIPY exhibits emission. Since the donor *meso*-aryl BODIPY emission at ~520 nm in both dyads **5** and **6** was completely quenched, we were not able to measure the quenched lifetimes of donor *meso*-aryl BODIPY with our experimental set-up. The fluorescence decays of both dyads **5** and **6** collected at their respective emission maxima of the *meso*-furyl BODIPY unit were fitted to a single exponential and the decay profile for dyad **6** at 630 nm is shown in Fig. 4. The lifetime data indicate that dyad **6** is more fluorescent than dyad **5** which is in agreement with the quantum yield data. We attribute this interesting observation tentatively to the restricted rotation of the *meso*-aryl BODIPY and *meso*-furyl BODIPY units in dyad **6** providing rigidity to the system and enhancing the radiative decay transitions. More studies are required to understand the unusual photophysical behavior of dyad **6**.

For understanding the reasons behind the distinct properties of the two BODIPY dyads, the *ab initio* calculations were performed using the DFT [23] method by adopting two different protocols as follows: (a) study of the HOMO–LUMO energy gap of compounds **5** and **6** and (b) study of HOMO–LOMO energies of the fragment of compounds **5** and **6** such as **10**, **11**, **12** and **13** (Chart 2). The contours of electronic distribution in HOMO and LUMO states on these molecules suggested significant differences between compounds **5** and **6**. For both the compounds, it was observed that the electron density in the HOMO state is located mainly in the *meso*-furyl BODIPY unit whereas the electron density is scattered over whole molecule in its LUMO state. However, as depicted in Fig. 5, the degree of delocalization of electron density in LUMO state is greater for compound **5** as compared to compound **6**.

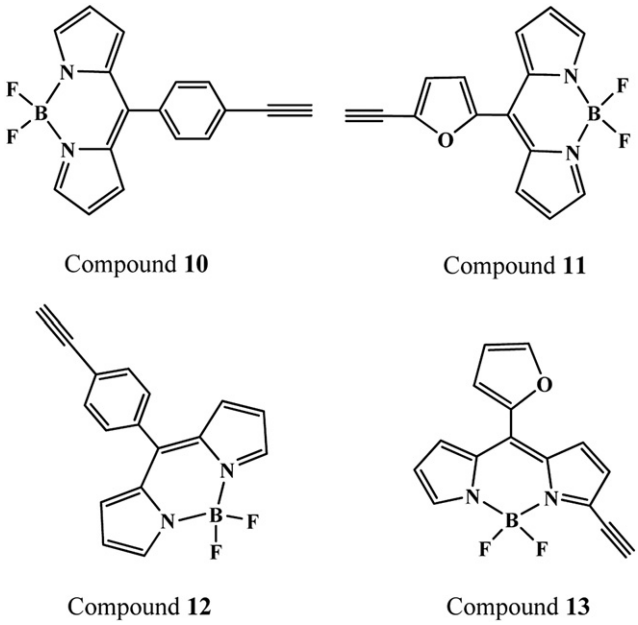


**Chart 2.** Structures of the fragments of two dyads **10**, **11**, **12,** and **13**.

To understand the efficiency and the direction of intramolecular energy transfer in dyads **5** and **6**, we have made use of a simplistic model involving a fragment based approach. In case of dyads, since they were synthesized as a result of association of two BODIPY

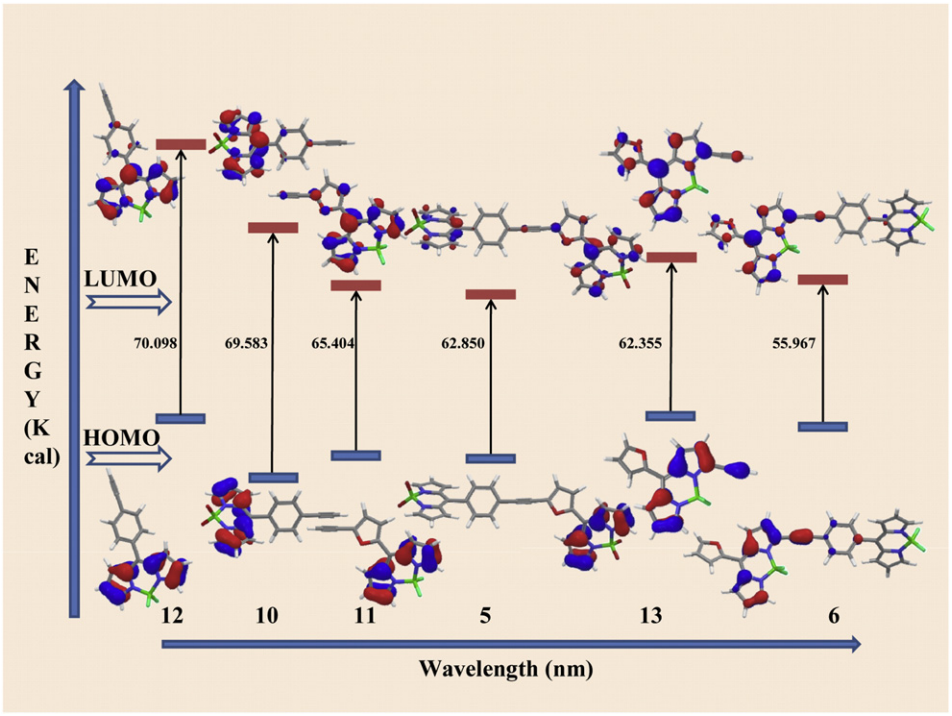


**Fig. 5.** The HOMO–LUMO states and energy gaps for compounds **5, 6** and their fragments.

units, for computational studies also, we followed the same path. Hence, the dyads **5** and **6** were sliced at their joining points to obtain fragments **10**, **11**, **12** and **13** and optimized for their geometry. However, the acetylene groups were intentionally kept attached (Chart 2). After initial optimization, the difference in energies was calculated with heats of formation (HF) of the species involved (*i.e.* $HF_{dyad} - HF_T - HF_F$), with the goal to compute stabilization or strain energy (SE). As shown in Table 2, the dyad systems are fairly destabilized/strained by almost 50 kcal than their individual monomers. There are several instances in the literature where correlations of strain energy have been established with the HOMO–LUMO energy gap of photoluminescent molecules [24,25]. These findings together give a hint that compound **5** experiences less strain and hence is more planar and having better π conjugation (Fig. 5) as compared to compound **6**. However, it does not reveal any information about the energy transfer in these systems. On the other hand, a difference in the energy gap of the two fragments could serve as a direct indicator of energy transferred and a sign of the value obtained would specify the direction. Table 2 and Fig. 5 also reveal that the energy gap for compound **6** is far less than the compound **5** (a difference of 6.88 kcal). On the contrary, the difference in the gap energies for the phenyl and furyl BODIPY fragments for compounds **5** and **6** clearly indicates that transfer of energy would occur from the *meso*-phenyl BODIPY portion to the *meso*-furyl BODIPY portion. To support this postulated direction of energy transfer and to shed further light on the process, excited state geometry optimization calculations were also performed with the TDDFT (Time-Dependent Density Functional Theory) method [26]. Ideally, the singlet–singlet type of energy transfer [27,28] process involves emission of energy from the excited state of the donor species which is absorbed by the ground state of the acceptor moiety. As shown in Fig. 5, the HOMO–LUMO gap of the excited state of the donor *meso*-phenyl BODIPY (compounds **14** and **15**) portion is also larger than the *meso*-furyl BODIPY portion in their ground states (compounds **11** and **13**). A keen observation of the HOMO–LUMO energy gaps and the TDDFT excitations energy data

**Table 2**
Computational data for compounds **5, 6** and their fragments **10**–**15**.

| Molecules | Heat of formation (HF)[c] | $\Delta G$[a] | HOMO[a] | LUMO[a] | Gap energies[a] | ET from T to F portion[a, d] | SE[c,e] | Excitation energy[a] ($\lambda_{abs}$[b]) |
|---|---|---|---|---|---|---|---|---|
| Compound **5** | −1646.04 | −40.29 | −145.404 | −82.554 | 62.850 | −4.18 | 50.12 | 60.42 (473.14) |
| Compound **6** | −1635.89 | −39.59 | −138.069 | −82.10 | 55.967 | −7.74 | 59.21 | 55.07 (519.19) |
| Compound **10** | −839.86 | −29.26 | −144.965 | −75.382 | 69.583 | – | – | 76.60 (373.25) |
| Compound **11** | −856.30 | −28.20 | −144.068 | −78.663 | 65.404 | – | – | 70.66 (404.57) |
| Compound **12** | −839.30 | −27.56 | −136.990 | −66.892 | 70.098 | – | – | 76.66 (372.92) |
| Compound **13** | −855.81 | −27.98 | −131.926 | −69.571 | 62.355 | – | – | 69.77 (409.78) |
| Compound **14** | −839.86 | −27.56 | −137.002 | −66.898 | 70.104 | – | – | – |
| Compound **15** | −839.29 | −27.60 | −136.996 | −66.816 | 70.180 | – | – | – |

Note: T and F refers to phenyl BODIPY and furyl BODIPY portions.
[a] Values in kcal.
[b] Wavelengths in nm.
[c] Values in Hartree.
[d] Calculated as: HOMO–LUMO $GAP_T$ – HOMO–LUMO $GAP_F$.
[e] Calculated as: $HF_{dyad} - HF_T - HF_F$.

(Table 2) suggests that these results are in concurrence with experimental outputs.

It is noteworthy that we have tried to compare the energies of the systems for calculation of SE (Stabilization or Strain Energy) which are not equivalent in terms of number of atoms. The result obtained leads us to believe that this fragment based approach has worked well in the case of BODIPY dyads. The values for difference of strain energies ($\Delta SE = SE_{dyad6} - SE_{dyad5} = 9.1$ Hartree) as calculated above from heats of formation of fragments and dyads are in close agreement with directly estimated value *i.e.* $\Delta SE = HF_{dyad6} - HF_{dyad5}$ (10.1 Hartree). Thus, from the computational studies, it is clear that the dyad **6** experiences greater strain, which results in a smaller gap energy hence bathochromic shift in absorption spectra. In addition, it also exhibits lesser degree of resonance in electron density as compared to dyad **5**. By virtue of all these factors, we conclude that there is a possibility of efficient intramolecular energy transfer from the *meso*-phenyl BODIPY unit to the *meso*-furyl BODIPY unit in dyads **5** and **6**.

## 4. Conclusions

In conclusion, we have synthesized two covalently linked BODIPY dyads containing the *meso*-phenyl BODIPY and the *meso*-furyl BODIPY units connected via *meso-meso* and *meso-α* positions using appropriate BODIPY building blocks under mild Pd(0) coupling conditions. In these dyads, the *meso*-phenyl BODIPY unit absorbs at higher energy and the *meso*-furyl BODIPY unit absorbs at lower energy which is clearly reflected in their absorption spectra. The steady state fluorescence spectra recorded by exciting the *meso*-phenyl BODIPY unit showed emission only from the *meso*-furyl BODIPY unit supporting singlet–singlet energy transfer from the *meso*-phenyl BODIPY unit to the *meso*-furyl BODIPY unit in both the dyads. Interestingly, the *meso-α* linked BODIPY dyad is more fluorescent than its corresponding BODIPY monomers unlike *meso-meso* linked BODIPY dyad which is weakly fluorescent. The computational studies supported the experimental results. The HOMO–LUMO gap energies of the dyads and their fragments indicated that for both *meso-meso* and *meso-α* linked BODIPY dyads, there would be energy transfer and the direction of energy transfer is from the *meso*-phenyl BODIPY unit to the *meso*-furyl BODIPY unit in both the dyads.

## Acknowledgment

MR thanks Department of Atomic Energy (DAE) for financial support and TKK thanks Indian Institute of technology for the fellowship. Authors thank Dr. Evans C. Coutinho, Bombay College of Pharmacy, for his valuable inputs.

## Appendix A. Supplementary information

Supporting information associated with this article can be found in the online version at doi:10.1016/j.dyepig.2011.12.002.

## References

[1] Hu X, Damjanovic A, Ritz T, Schulten K. Architecture and mechanism of the light-harvesting apparatus of purple bacteria. Proc Natl Acad Sci USA 1998; 95(11):5935–41.
[2] Loudet A, Burgess K. BODIPY dyes and their derivatives: syntheses and spectroscopic properties. Chem Rev 2007;107(11):4891–932.
[3] Ulrich G, Ziessel R, Harriman A. The chemistry of fluorescent bodipy dyes: versatility unsurpassed. Angew Chem Int Ed 2008;47(7):1184–201.
[4] Ziessel R, Ulrich G, Harriman A. The chemistry of Bodipy: a new El Dorado for fluorescence tools. New J Chem 2007;31(4):496–501.
[5] Wagner RW, Lindsey JS. A molecular photonic wire. J Am Chem Soc 1994; 116(21):9759–60.
[6] Li F, Yang SI, Ciringh Y, Seth J, Martin Iii CH, Singh DL, et al. Design, synthesis, and photodynamics of light-harvesting arrays comprised of a porphyrin and one, two, or eight boron-dipyrrin accessory pigments. J Am Chem Soc 1998; 120(39):10001–17.
[7] Ravikanth M, Agarwal N, Kumaresan D. Synthesis of energy donors appended dithiaporphyrin systems. Chem Lett 2000;29(7):836–7.
[8] Kumaresan D, Gupta I, Ravikanth M. Synthesis of 21-oxoporphyrin building blocks and energy donor appended systems. Tetrahedron Lett. 2001;42(48): 8547–50.
[9] Ziessel R, Goze C, Ulrich G. Design and synthesis of alkyne-substituted boron in dipyrromethene frameworks. Synthesis 2007;6:936–49.
[10] Goeb S, Ziessel R. Synthesis of novel tetrachromophoric cascade-type Bodipy dyes. Tetrahedron Lett. 2008;49(16):2569–74.
[11] Wan CW, Burghart A, Chen J, Bergström F, Johansson LBÅ, Wolford MF, et al. Anthracene-BODIPY cassettes: syntheses and energy transfer. Chem Eur J 2003;9(18):4430–41.
[12] Bröring M, Krüger R, Link S, Kleeberg C, Kohler S, Xie X, et al. Bis(BF2)-2,2′-bidipyrrins (BisBODIPYs): highly fluorescent BODIPY dimers with large stokes shifts. Chem Eur J 2008;14(10):2976–83.
[13] Goze C, Ulrich G, Charbonnière L, Cesario M, Prange T, Ziessel R. Cation sensors based on terpyridine functionalized boradiazaindacene. Chem Eur J 2003; 9(16):3748–55.
[14] Galletta M, Campagna S, Quesada M, Ulrich G, Ziessel R. The elusive phosphorescence of pyrromethene-BF2 dyes revealed in new multicomponent species containing Ru (ii)-terpyridine subunits. Chem Commun 2005;33: 4222–4.
[15] Harriman A, Izzet G, Ziessel R. Rapid energy transfer in cascade-type Bodipy dyes. J Am Chem Soc 2006;128(33):10868–75.
[16] Barin G, Yilmaz MD, Akkaya EU. Boradiazaindacene (Bodipy)-based building blocks for the construction of energy transfer cassettes. Tetrahedron Lett 2009;50(15):1738–40.
[17] Zhang X, Xiao Y, Qian X. Highly efficient energy transfer in the light harvesting system composed of three kinds of boronâ dipyrromethene derivatives. Org Lett 2008;10(1):29–32.
[18] Bura T, Retailleau P, Ziessel R. Efficient Synthesis of panchromatic dyes for energy concentration. Angew Chem Int Ed. 2010;49(37):6659–63.
[19] Diring S, Puntoriero F, Nastasi F, Campagna S, Ziessel R. Star-shaped multichromophoric arrays from BODIPY dyes grafted on truxene core. J Am Chem Soc 2009;131(17):6108–10.
[20] Kim K, Jo C, Easwaramoorthi S, Sung J, Kim DH, Churchill DG. Crystallographic, photophysical, NMR spectroscopic and reactivity manifestations of the "8-heteroaryl effect" in 4,4-difluoro-8-(C(4)H(3)X)-4-bora-3a,4a-diaza-s-indacene (X = O, S, Se) (BODIPY) systems. Inorg Chem 2010;49(11): 4881–94.
[21] Kim S, Ohulchanskyy TY, Baev A, Prasad PN. Synthesis and nanoparticle encapsulation of 3, 5-difuranylvinyl-boradiaza-s-indacenes for near-infrared fluorescence imaging. J Mater Chem 2009;19(20):3181–8.
[22] Khan TK, Pissurlenkar RRS, Shaikh MS, Ravikanth M. Synthesis and studies of covalently linked meso-furyl boron-dipyrromethene-ferrocene conjugates. J Organomet Chem 2012;697:65–73.
[23] Hohenberg P, Kohn W. Inhomogeneous electron gas. Phys Rev 1964;136(3B): B864–71.
[24] Peng XH, Alizadeh A, Bhate N, Varanasi KK, Kumar SK, Nayak SK. First-principles investigation of strain effects on the energy gaps in silicon nanoclusters. J Phys Condens Matter 2007;19:266212.
[25] Peng XH, Ganti S, Alizadeh A, Sharma P, Kumar SK, Nayak SK. Strain-engineered photoluminescence of silicon nanoclusters. Phys Rev B 2006;74(3): 035339.
[26] Runge E, Gross EKU. Density-functional theory for time-dependent systems. Phys Rev Lett. 1984;52(12):997–1000.
[27] Förster T. Transfer mechanisms of electronic excitation energy. Radiat Res Suppl; 1960:326–39.
[28] McNaught AD, Wilkinson A. Compendium of chemical terminology: the gold book. Second ed. Blackwell Science; 1997.
[29] Qin W, Leen V, Rohand T, Dehaen W, Dedecker P, Van der Auweraer M, et al. Synthesis, spectroscopy, crystal structure, electrochemistry, and quantum chemical and molecular dynamics calculations of a 3-anilino difluoroboron dipyrromethene dye. J Phys Chem A 2009; 113(2):439–47.
[30] Jaguar, version 7.8. New York, NY: Schrödinger, LLC; 2011.
[31] Rocks cluster v5.4 (Maverick). San Diego: Rocks Cluster Group, San Diego Supercomputer Center, University of California; 2010.
[32] Wagner RW, Lindsey JS. Boron-dipyrromethene dyes for incorporation in synthetic multi-pigment light-harvesting arrays. Pure Appl Chem. 1996;68(7): 1373–80.
[33] Stephens PJ, Devlin FJ, Chabalowski CF, Frisch MJ. Ab initio calculation of vibrational absorption and circular dichroism spectra using density functional force fields. J Phys Chem 1994;98(45):11623–7.
[34] Hariharan PC, Pople JA. Natural population analysis (NPA). Theor Chim Acta 1973;28:213–22.